Crystal Growth of a New Series of Complex Niobates, $LnKNaNbO_5$ (Ln = La, Pr, Nd, Sm, Eu, Gd, and Tb): Structural Properties and Photoluminescence

Irina P. Roof, Thomas-C. Jagau, Wolfgang G. Zeier, Mark D. Smith, and Hans-Conrad zur Loye*

University of South Carolina, Columbia, South Carolina 29208

Received February 4, 2009. Revised Manuscript Received March 16, 2009

Single crystals of $LnKNaNbO_5$ (Ln = La, Pr, Nd, Sm, Eu, Gd, Tb) were grown out of a reactive high temperature hydroxide melt. The structures were solved by single crystal X-ray diffraction. All compounds of the series $LnKNaNbO_5$ crystallize in the space group *P*4/*nmm*. The niobium is located in a rare square pyramidal coordination environment in this layered structure. $EuKNaNbO_5$, $GdKNaNbO_5$, and $TbKNaNbO_5$ exhibit room temperature photoluminescence with bright orange-red, pink-purple, and green emissions, respectively. Unlike in many oxide structures, the photoluminescence is not quenched, although the rare earth elements fully occupy a position in the crystal structure.

1. Introduction

Niobium-containing oxides comprise a large group of compounds with distinct structures that exhibit a wide range of interesting physical properties, such as high dielectric constants,[1−5] photocatalytic behavior,[6−14] and photoluminescence.[9,13,15−17] As a result of the increased interest in fabricating high quality, energy efficient light-emitting diodes (LEDs), complex photoluminescent oxides are increasingly being investigated. The main focus has been on doping such complex oxide structures with rare-earth-metal ions to achieve enhanced luminescent behavior via the rare earth cations, where the niobate structures influence the likely f−f and f−d transitions responsible for photoluminescence.[9,13,17,18] These optical properties are greatly dependent on the composition and, perhaps more importantly, on the details of the material's crystal structure. For these reasons there has been a push to prepare new niobate materials with new crystal structures and, thus, potentially new or enhanced properties. One approach to the discovery of such phases, as described in this paper, is the exploration of phase space via single crystal growth of new compositions/structures out of molten hydroxide fluxes.[19−25]

The acid−base chemistry of molten hydroxide fluxes, best described by the Lux−Flood concept of oxoacidity,[26,27] allows a wide range of cationic species to be present in solution, an essential condition for their eventual incorporation into single crystals. In the Lux−Flood concept of oxoacidity, the autodissociation of water, and the analogous autodissociation of molten hydroxides yield the following equations:

$$2H_2O \rightleftarrows H_3O^+ + OH^- \quad (1)$$

$$2OH^- \rightleftarrows H_2O + O^{2-} \quad (2)$$

By analogy with the autodissociation of water (eq 1), where H_3O^+ is the acidic and OH^- the basic species, in a hydroxide melt (eq 2), H_2O is the acidic and O^{2-} is the basic species. Adding water, consequently, increases the acidity

* To whom correspondence should be addressed. Tel: +1-803-777-6916. Fax: +1-803-777-8508. E-mail: zurloye@mail.chem.sc.edu.

(1) Kan, A.; Ogawa, H.; Yokoi, A.; Nakamura, Y. *J. Eur. Ceram. Soc.* **2007**, *27*, 2977.
(2) Kharitonova, E. P.; Voronkova, V. I.; Yanovski, V. K.; Stefanovich, S. Y. *J. Cryst. Growth* **2002**, *237*, 703.
(3) Nobre, M. A. L.; Lanfredi, S. *Catal. Today* **2003**, *78*, 529.
(4) Sebastian, M. T.; Solomon, S.; Ratheesh, R.; George, J.; Mohanan, P. *J. Am. Ceram. Soc.* **2001**, *84*, 1487.
(5) Solomon, S.; Joseph, J. T.; Kumar, H. P.; Thomas, J. K. *Mater. Lett.* **2006**, *60*, 2814.
(6) Abe, R.; Higashi, M.; Zou, Z.; Sayama, K.; Abe, Y.; Arakava, H. *J. Phys. Chem. B* **2004**, *108*, 811.
(7) Blasse, G. *J. Solid State Chem.* **1988**, *72*, 72.
(8) Blasse, G.; Lammers, M. J. J.; Verhaar, H. C. G.; Brixner, L. H.; Torardi, C. C. *J. Solid State Chem.* **1985**, *60*, 258.
(9) Yu, C. C.; Liu, X. M.; Yu, M.; Lin, C. K.; Li, C. X.; Wang, H.; Lin, J. *J. Solid State Chem.* **2007**, *180*, 3058.
(10) Zhang, G.; Gong, J.; Zou, X.; Fangsheng, H.; Zhang, H.; Zhang, Q.; Liu, Y.; Yang, X.; Hu, B. *Chem. Eng. J.* **2006**, *123*, 59.
(11) Zhang, G.; He, F.; Zou, X.; Gong, J.; Tu, H.; Zhang, H.; Zhang, Q.; Liu, Y. *J. Alloys Compd.* **2007**, *425*, 82.
(12) Zhang, G.; Zou, X.; Gong, J.; He, F.; Zhang, H.; Zhang, Q.; Liu, Y.; Yang, X.; Hu, B. *J. Alloys Compd.* **2006**, *425*, 76.
(13) Zhou, Y.; Lu, M.; Qiu, Z.; Zhang, A.; Ma, Q.; Zhang, H.; Yang, Z. *Mater. Sci. Eng. B* **2007**, *140*, 128.
(14) Zou, Z.; Ye, J.; Arakava, H. *Mater. Res. Bull.* **2001**, *36*, 1185.
(15) Liu, X. M.; Lin, J. *J. Lumin.* **2007**, *122−123*, 700.
(16) Srivastava, A. M.; Ackermann, J. F.; Beers, W. W. *J. Solid State Chem.* **1997**, *134*, 187.
(17) Wen, C. H.; Chu, S. Y.; Shin, Y. Y.; Lee, C. T.; Juang, Y. D. *J. Alloys Compd.* **2008**, *459*, 107.
(18) Sivakumar, V.; Varadaraju, U. V. *J. Solid State Chem.* **2008**, *181*, 3344.
(19) Davis, M. J.; Mugavero III, S. J.; Glab, K. I.; Smith, M. D.; zur Loye, H.-C. *Solid State Sci.* **2004**, *6*, 413.
(20) Gemmill, W. R.; Smith, M. D.; zur Loye, H.-C. *J. Solid State Chem.* **2006**, *179*, 1750.
(21) Mugavero III, S. J.; Smith, M. D.; zur Loye, H.-C. *J. Solid State Chem.* **2005**, *178*, 200.
(22) Roof, I. P.; Park, S.; Vogt, T.; Rassolov, V.; Smith, M. D.; Omar, S.; Nino, J.; zur Loye, H.-C. *Chem. Mater.* **2008**, *20*, 3327.
(23) Roof, I. P.; Smith, M. D.; Cussen, E. J.; zur Loye, H.-C. *J. Solid State Chem.* **2009**, *182*, 295.

10.1021/cm9003245 CCC: $40.75 © 2009 American Chemical Society
Published on Web 04/14/2009

Table 1. Crystal and Structural Refinement Data for $LnKNaNbO_5$

	Empirical Formula					
	$PrKNaNbO_5$	$NdKNaNbO_5$	$SmKNaNbO_5$	$EuKNaNbO_5$	$GdKNaNbO_5$	$TbKNaNbO_5$[a]
formula weight (g/mol)	375.91	379.24	385.35	386.96	392.25	391.92
space group	*P4/nmm*	*P4/nmm*	*P4/nmm*	*P4/nmm*	*P4/nmm*	*P4/nmm*
a (Å)	5.7525(1)	5.7285(2)	5.69670(10)	5.68540(10)	5.6714(1)	5.6504(4)
c (Å)	8.2405(2)	8.2339(5)	8.2210(3)	8.2157(3)	8.2161(2)	8.2077(9)
V (Å^3)	272.688(9)	270.20(2)	266.791(12)	265.562(12)	264.269(9)	262.055(7)
Z	2	2	2	2	2	
density (calculated, Mg/m^3)	4.578	4.661	4.797	4.839	4.929	
absorption coefficient (mm^{-1})	11.705	12.404	13.837	14.655	15.407	
F(000)	340	342	346	348	350	
crystal size (mm^3)	0.06 × 0.05 × 0.04	0.08 × 0.06 × 0.03	0.07 × 0.04 × 0.04	0.04 × 0.04 × 0.03	0.06 × 0.06 × 0.02	
Θ range	2.47−40.27°	2.47−40.22°	2.48−40.25°	2.48−40.27°	2.48−40.21°	
reflections collected	8309	7006	7517	6749	7054	
independent reflections	544 (R_{int} = 0.0313)	536 (R_{int} = 0.0314)	532 (R_{int} = 0.0280)	531 (R_{int} = 0.0442)	527 (R_{int} = 0.0315)	
ref. used for unit cell parameters	3395	3244	3959	1932	3193	
completeness to Θ_{max}	100.0%	99.8%	99.8%	100.0%	100.0%	
goodness-of-fit on F^2	1.104	1.165	1.077	1.107	1.080	
R indices (all data)	R_1 = 0.0215	R_1 = 0.0105	R_1 = 0.0271	R_1 = 0.0392	R_1 = 0.0203	
	wR_2 = 0.0448	wR_2 = 0.0434	wR_2 = 0.0454	wR_2 = 0.0678	wR_2 = 0.0419	
largest diff. peak and hole (e$^-$/Å^{-3})	0.966 and −1.407	0.906 and −1.580	1.122 and −1.187	2.778 and −1.673	0.898 and −1.125	

[a] The data for $TbKNaNbO_5$ was obtained from a Le Bail fit of the powder X-ray diffraction data.

of the hydroxide melt, whereas drying the melt, for example, by employing an open reaction vessel to enable the evaporation of water during the time of the reaction, increases the basicity. Since the solubility of metal oxides in molten hydroxides is strongly dependent on the melt's acidity,[20−22,28] controlling the water content of the reaction controls the solubility of the reactant species.

We have been exploring the use of hydroxide melts for the preparation of novel niobates and have been pursuing the preparation of new oxides with unusual and promising physical properties. We have previously communicated synthesis, structural characterization, and unusual room temperature photoluminescence of $EuKNaTaO_5$.[25] Expanding such efforts has resulted in this series of complex niobium oxides, $LnKNaNbO_5$ (Ln = La, Pr, Nd, Sm, Eu, Gd, Tb), and the exploration of their photoluminescence properties. The synthesis of $LaKNaNbO_5$ had already been reported by Liao et al.,[29] and consequently, we focused on expanding the range of known compositions and on establishing the size limit of the smaller rare earths that could be accommodated by this structure type.

The vast majority of transition metals in oxides are found in either tetrahedral or octahedral coordination environments. A smaller subset is known to take on square planar coordination, and only very few are found in square pyramidal coordination environments. Most complex niobium oxides contain niobium in octahedral coordination;[11,18,30] however, a few compositions, such as Ln_2KNbO_6 (Ln = La, Nd)[22] and $NaRbLnNbO_5$ (Ln = La, Nd, Sm, Eu, Gd),[31] contain niobium in a square pyramidal coordination environment. The title compounds, $LnKNaNbO_5$ (Ln = La, Pr, Nd, Sm, Eu, Gd, Tb), also contain niobium in a square pyramidal coordination environment. Herein, we report on the single crystal growth of a new series of complex niobates, $LnKNaNbO_5$ (Ln = La, Pr, Nd, Sm, Eu, Gd, Tb), using

Table 2. Atomic Coordinates and Equivalent Isotropic Displacement Parameters U_{eq} (Å^2) for $LnKNaNbO_5$[a]

	x	*y*	*z*	U_{eq}
		$PrKNaNbO_5$		
Pr(1)	3/4	1/4	1/2	0.008(1)
Na(1)	1/4	1/4	0.7592(2)	0.011(1)
K(1)	3/4	1/4	0	0.025(1)
Nb(1)	1/4	1/4	0.2565(1)	0.007(1)
O(1)	0.0204(2)	0.0204(2)	0.3271(2)	0.011(1)
O(2)	1/4	1/4	0.0346(4)	0.016(1)
		$NdKNaNbO_5$		
Nd(1)	3/4	1/4	1/2	0.008(1)
Na(1)	1/4	1/4	0.7592(2)	0.012(1)
K(1)	3/4	1/4	0	0.025(1)
Nb(1)	1/4	1/4	0.2574(1)	0.007(1)
O(1)	0.0200(2)	0.0200(2)	0.3283(2)	0.012(1)
O(2)	1/4	1/4	0.0352(4)	0.016(1)
		$SmKNaNbO_5$		
Sm(1)	3/4	1/4	1/2	0.008(1)
Na(1)	1/4	1/4	0.7593(2)	0.011(1)
K(1)	3/4	1/4	0	0.025(1)
Nb(1)	1/4	1/4	0.2591(1)	0.007(1)
O(1)	0.0189(1)	0.0189(1)	0.3304(2)	0.012(1)
O(2)	1/4	1/4	0.0364(3)	0.017(1)
		$EuKNaNbO_5$		
Eu(1)	3/4	1/4	1/2	0.009(1)
Na(1)	1/4	1/4	0.7597(4)	0.013(1)
K(1)	3/4	1/4	0	0.025(1)
Nb(1)	1/4	1/4	0.2598(1)	0.007(1)
O(1)	0.0190(3)	0.0190(3)	0.3307(4)	0.013(1)
O(2)	1/4	1/4	0.0360(7)	0.015(1)
		$GdKNaNbO_5$		
Gd(1)	3/4	1/4	1/2	0.008(1)
Na(1)	1/4	1/4	0.7599(2)	0.012(1)
K(1)	3/4	1/4	0	0.025(1)
Nb(1)	1/4	1/4	0.2606(1)	0.007(1)
O(1)	0.0183(2)	0.0183(2)	0.3320(2)	0.012(1)
O(2)	1/4	1/4	0.0376(4)	0.016(1)

[a] U_{eq} is defined as one third of the trace of the orthogonalized U_{ij} tensor.

(24) Roof, I. P.; Smith, M. D.; zur Loye, H.-C. *J. Cryst. Growth* **2008**, *1*, 310–240.
(25) Roof, I. P.; Smith, M. D.; Park, S.; zur Loye, H.-C. *J. Am. Chem. Soc.* **2009**, *131*, 4202.
(26) Flood, H.; Fortland, T. *Acta Chem. Scand.* **1947**, *1*, 592.
(27) Lux, H. Z. Z. *Electrochemistry* **1939**, *45*, 303.
(28) Keller, S. W.; Carlson, V. A.; Sandford, D.; Stenzel, F.; Stacy, A. M.; Kwei, G. H.; Alario-Franco, M. *J. Am. Chem. Soc.* **1994**, *116*, 8070.
(29) Laio, J.-H.; Tsai, M.-C. *Cryst. Growth Des.* **2002**, *2*, 83.
(30) Liu, J. W.; Chen, G.; Li, Z. H.; Zhang, Z. G. *Int. J. Hydrogen Energy* **2007**, *32*, 2269.
(31) Cavazos, R. J.; Schaak, R. E. *Mater. Res. Bull.* **2004**, *39*, 1209.

Table 3. Selected Interatomic Distances (Å) for $LnKNaNbO_5$

	$PrKNaNbO_5$	$NdKNaNbO_5$	$SmKNaNbO_5$	$EuKNaNbO_5$	$GdKNaNbO_5$
Nb−O(1) × 4	1.9567(15)	1.9525(15)	1.9519(12)	1.947(3)	1.9487(14)
Nb−O(2) × 1	1.829(3)	1.830(3)	1.831(3)	1.838(6)	1.832(3)
Ln−O(1) × 8	2.4887(10)	2.4755(10)	2.4542(9)	2.4490(18)	2.4386(11)
K−O(1) × 8	3.3808(14)	3.3813(14)	3.3850(12)	3.383(3)	3.3889(15)
K−O(2) × 4	2.8903(3)	2.8788(3)	2.8640(3)	2.8580(6)	2.8525(4)
Na−O(1) × 4	2.3116(16)	2.3029(16)	2.2884(13)	2.287(3)	2.2809(16)
Na−O(2) × 1	2.269(4)	2.272(4)	2.278(3)	2.270(6)	2.282(4)

reactive hydroxide fluxes, their structure determination, and their photoluminescence properties.

2. Experimental Section

2.1. Sample Preparation. *Single Crystals.* Single crystals of $LnKNaNbO_5$ (Ln = La, Pr, Nd, Sm, Eu, Gd, Tb) were grown out of a reactive eutectic melt of potassium and sodium hydroxides. Commercially available alkali metal hydroxides, typically containing approximately 15% water by weight, were used. All reactions were carried out in silver tubes approximately 8 cm long and with a 1.25 cm diameter, which had been flame-sealed at one end. The rare earth sesquioxides Ln_2O_3 (Ln = La, Nd, Sm, Eu, Gd; Alfa Aesar Reacton, 99.9%) were activated at 1000 °C for 24 h. Pr_2O_3 and Tb_2O_3 were obtained by reducing Pr_6O_{11} and Tb_4O_7, respectively (Alfa Aesar Reacton, 99.9%) with a hydrogen/nitrogen gas flow at 1000 °C for 24 h. Nb_2O_5 (Alfa Aesar Puratronic, 99.9985%), NaOH (Fisher, ACS reagent), and KOH (Mallinckrodt Chemicals) were used as received.

Depending on the reactivity of the lanthanide, optimal ratios of starting materials, namely, Ln_2O_3 and Nb_2O_5, were determined. For the preparation of $LnKNaNbO_5$ (Ln = La, Pr, Nd, Sm, Eu), 0.5 mmol of Ln_2O_3 and 0.5 mmol of Nb_2O_5 were used, whereas for the successful syntheses of $GdKNaNbO_5$ and $TbKNaNbO_5$ a ratio of 2:1 of the appropriate rare earth oxide, Ln_2O_3 and Nb_2O_5, was necessary. Furthermore, the amount of hydroxide flux had to be adjusted to the specific rare earth as well. For the preparation of $LnKNaNbO_5$ (Ln = La, Nd, Sm, Eu) 2.0 g of KOH and 2.0 g of NaOH were used. The synthesis of $PrKNaNbO_5$ was performed in a mixture of 1.6 g of NaOH and 2.3 g of KOH, and that of $GdKNaNbO_5$ in a mixture of 2.0 g of NaOH and 2.8 g of KOH.

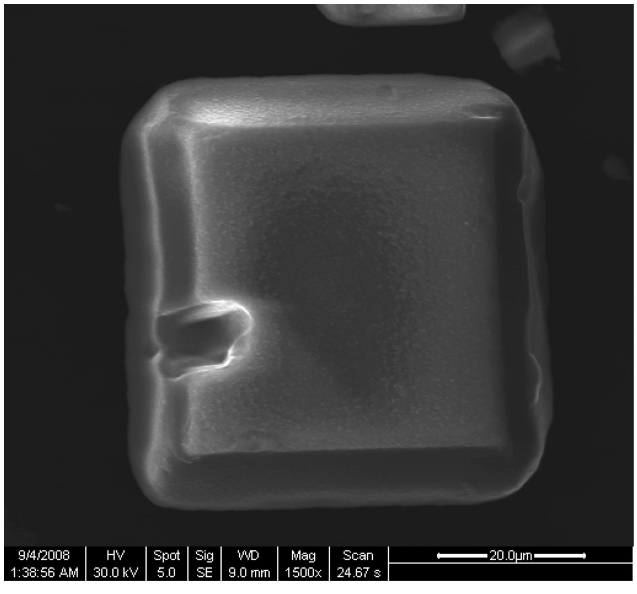

Figure 1. ESEM image of a typical single crystal of $LaKNaNbO_5$, representative of the $LnKNaNbO_5$ (Ln = La, Pr, Nd, Sm, Eu, Gd, Tb) series.

For the preparation of $EuKNaNbO_5$ and $PrKNaNbO_5$ an additional 1.0 g of deionized water was added to the reaction mixtures to increase the acidity of the system for the optimal dissolution of the starting metal oxides.

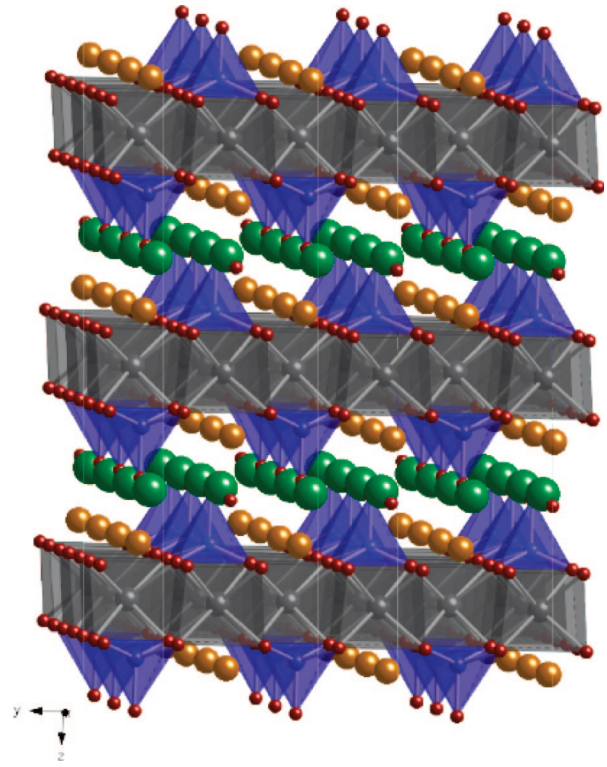

Figure 2. Schematic of the crystal structure of $LnKNaNbO_5$ (Ln = La, Pr, Nd, Sm, Eu, Gd, Tb) viewed along the *x*-axis. LnO_8 distorted cubes are shown in gray; NbO_5 square pyramids are in blue; K^+, Na^+, and O^{2-} are green, brown, and red spheres, respectively.

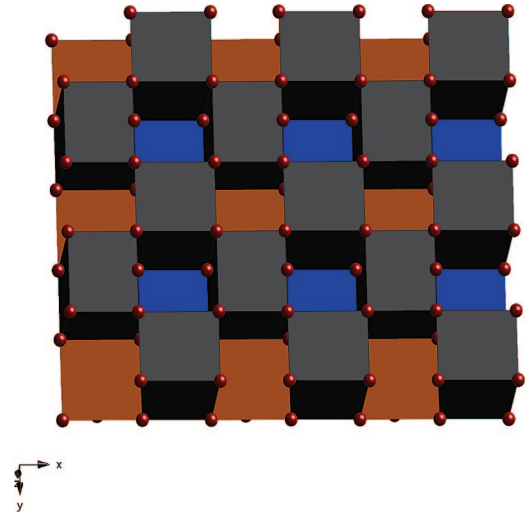

Figure 3. Checkerboard pattern of the polyhedra within the layers of $LnKNaNbO_5$ (Ln = La, Pr, Nd, Sm, Eu, Gd, Tb).

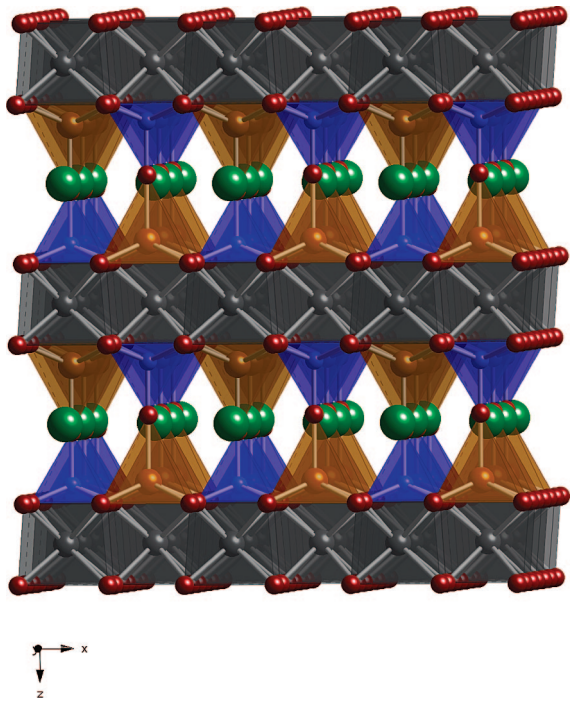

Figure 4. Crystal structure of $LnKNaNbO_5$ (Ln = La, Pr, Nd, Sm, Eu, Gd, Tb) emphasizing the interconnectivity of the NbO_5 (shown in blue) and NaO_5 (shown in yellow) square pyramids.

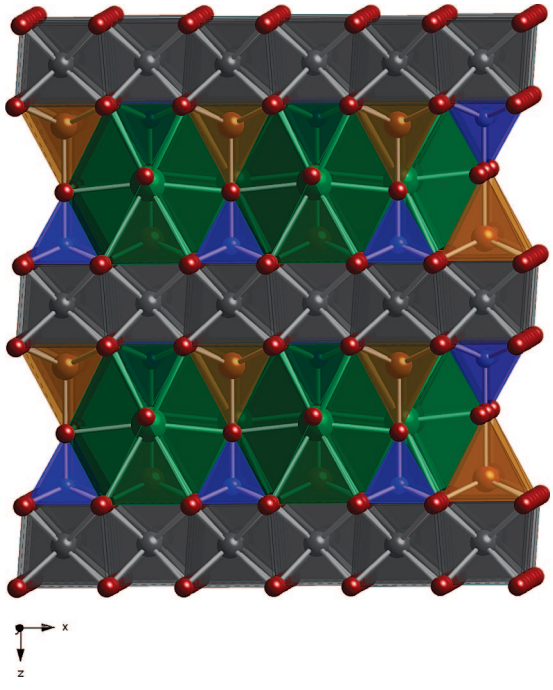

Figure 5. Polyhedral view of $LnKNaNbO_5$ (Ln = La, Pr, Nd, Sm, Eu, Gd, Tb) showing the potassium polyhedra (shown in green) between the sheets of $NaLnNbO_5$.

After loading the reagents into the vessel, the silver tube was crimped shut and folded over twice before being placed upright in to a box furnace. For $LaKNaNbO_5$ and $NdKNaNbO_5$ the system was heated to 600 °C at a rate of 10 °C/min and held at the target temperature for 24 h. Then, the furnace was shut off and allowed to cool to room temperature. For $PrKNaNbO_5$ the reaction was carried out at 400 °C for 24 h using the same heating rate, whereas a target temperature of 450 °C was applied for the preparation of $SmKNaNbO_5$, $EuKNaNbO_5$, and $GdKNaNbO_5$. These reaction conditions led to the formation of pure single crystal samples of the desired phases.

Crystals of $LnKNaNbO_5$ were isolated by dissolving the hydroxide flux with deionized water aided by sonication. All crystals were colorless except for the Nd compound which was distinctly blue and the Sm and Eu compounds which were pale yellow and pale pink, respectively. The polycrystalline powders were of the same colors as the crystals (vide infra).

Polycrystalline Powders. Powder samples of $LnKNaNbO_5$ (Ln = La, Pr, Nd, Sm, Eu, Gd, Tb) were obtained by classical solid-state synthesis starting from Nb_2O_5 (Alfa Aesar Puratronic, 99.9985%), Ln_2O_3 (Alfa Aesar REacton, 99.9%, activated at 1000 °C for 24 h prior to use), Na_2CO_3 (Mallinckrodt Chemicals, dried at 120 °C) and K_2CO_3 (Fisher ACS reagent, dried at 120 °C). In a typical procedure stoichiometric amounts of all reagents (5% excess of K_2CO_3 and Na_2CO_3) were thoroughly ground together and loaded into an alumina boat. The mixture was heated three times for 6 h using a heating rate of 10 °C/min, first to 750 °C, then to 800 °C, and finally, to 850 °C. After every heat treatment the furnace was shut off and allowed to cool to room temperature so that the reaction mixture could be reground. The synthesis of $TbKNaNbO_5$ powder was carried out under a nitrogen gas flow to avoid the oxidation of terbium. The powder samples contained small amounts of Ln_3NbO_7, and the amount of this impurity increased from La to Tb. We did not observe the formation of $NaNbO_3$ or $KNbO_3$, neither with the solid-state reactions nor with the crystal growth. Heating the powders to temperatures in excess of 850 °C will lead to sample decomposition and the formation of the Ln_3NbO_7 phases.

2.2. Characterization. *Single Crystal X-ray Diffraction.* X-ray intensity data of all compounds of the series $LnKNaNbO_5$, except the known lanthanum analogue, were collected at 294(2) K on a Bruker SMART APEX diffractometer (Mo Kα radiation, λ = 0.71073 Å). Raw area detector data frame integration was carried out with SAINT+.[32] Final unit cell parameters were determined by least-squares refinement of reflections harvested from the data sets (Table 1). The data were corrected for absorption effects with SADABS.[32] Direct methods structure solution, difference Fourier calculations, and full-matrix least-squares refinement against F^2 were performed with SHELXTL.[33]

All compounds of the series $LnKNaNbO_5$ crystallize in the space group *P*4/*nmm*. This was determined by the solutions and refinements of the structures. The asymmetric unit contains six atoms: one lanthanide atom, one niobium atom, one potassium atom, one sodium atom, and two oxygen atoms. All atoms lie on special positions. The rare earth atom is located on a 4-fold rotoinversion axis combined with a crystallographic mirror plane and a 2-fold axis (Wyckoff site 2b). The potassium atom also resides on a 4-fold rotoinversion axis combined with a mirror plane and a 2-fold axis (Wyckoff site 2a). The niobium, the sodium, and the oxygen O(2) atoms lie on a 4-fold axis of rotation. Moreover, these three atoms reside on two mirror planes (Wyckoff sites 2c). The residual oxygen atom O(1) is located on a simple mirror plane (Wyckoff site 8j). All atoms were refined with anisotropic displacement parameters. The most important crystallographic data from the single crystal structure refinements for $LnKNaNbO_5$ are found in Table 1. Atomic positions and selected interatomic distances are shown in Tables 2 and 3, respectively.

Powder X-ray Diffraction. Powder X-ray diffraction patterns were collected on a Rigaku Dmax/2100 powder diffractometer using Cu Kα radiation. Data were collected in 0.04° steps over the 2θ range of 5−70°.

(32) *SMART*, Version 5.625; *SAINT+*, Version 6.45; and *SADABS*, Version 2.05; Bruker Analytical X-ray Systems, Inc.: Madison, WI, 2001.

Table 4. Bond Valence Sums for $LnKNaNbO_5$

	$LaKNaNbO_5$	$PrKNaNbO_5$	$NdKNaNbO_5$	$SmKNaNbO_5$	$EuKNaNbO_5$	$GdKNaNbO_5$
Ln	3.10	3.10	2.93	2.97	2.90	2.92
Na	1.23	1.30	1.32	1.35	1.36	1.37
Nb	4.76	4.78	4.82	4.83	4.85	4.85

UV−Visible Spectrometry. Diffuse-reflectance spectra of both ground crystals and polycrystalline powder samples of all compounds of the $LnKNaNbO_5$ series were obtained using a Perkin Elmer Lambda 35 UV/vis scanning spectrophotometer equipped with an integrating sphere. The raw data were converted from reflection to absorbance by the use of the Kubelka−Munk function. The optical band gap energy was estimated using the onset of the absorption edge.

Luminescence. The excitation and emission spectra for $GdKNaNbO_5$, $EuKNaNbO_5$, and $TbKNaNbO_5$ were collected at room temperature on ground crystals using a Perkin Elmer LS 55 fluorescence spectrometer. The other compositions containing La, Pr, Nd, and Sm did not visibly luminesce and were, thus, not measured.

3. Results and Discussion

Crystal Structure. Hydroxide melts are known to be an excellent medium for preparing single crystals of lanthanide containing complex oxides.[34] In the case of $LnKNaNbO_5$ the "acidic" flux of NaOH and KOH acted as both a solvent and a reactant. Since controlling the acidity of the melt is an essential component to the successful dissolution and subsequent recrystallization of the constituents, the dehydration of the melt was minimized by performing the crystal growth process in sealed silver tubes. A SEM micrograph of a typical rectangular crystal of $LaKNaNbO_5$ is shown in Figure 1.

All compounds of the series $LnKNaNbO_5$ (Ln = La, Pr, Nd, Sm, Eu, Gd, Tb) crystallize in the tetragonal space group *P*4/*nmm*. A schematic of the crystal structure viewed along the *x*-axis is found in Figure 2. The structure type was first reported by Liao and Tsai[29] and can be best understood as a layered structure. Each layer consists of edge-sharing LnO_8 cubes that form a checkerboard pattern as shown in Figure 3. Groups of four edge-sharing cubes of LnO_8 are further edge-shared to the four basal edges of NbO_5 and NaO_5 square pyramids located above and below a vacant cube on opposite sides of the sheet, where the NbO_5 and NaO_5 square pyramids are arranged in alternating rows. Each NbO_5 and NaO_5 square pyramid shares its apical oxygen with a NaO_5 and NbO_5, respectively, square pyramid on the adjacent layer (Figure 4). The potassium ions occupy the space between the $NaLnNbO_5$ sheets, where each potassium ion is surrounded by 12 oxygen atoms, four apical oxygen atoms of two NbO_5 and two NaO_5 pyramids and eight oxygens belong to two LnO_8 cubes in adjacent layers as can be seen in Figure 5.

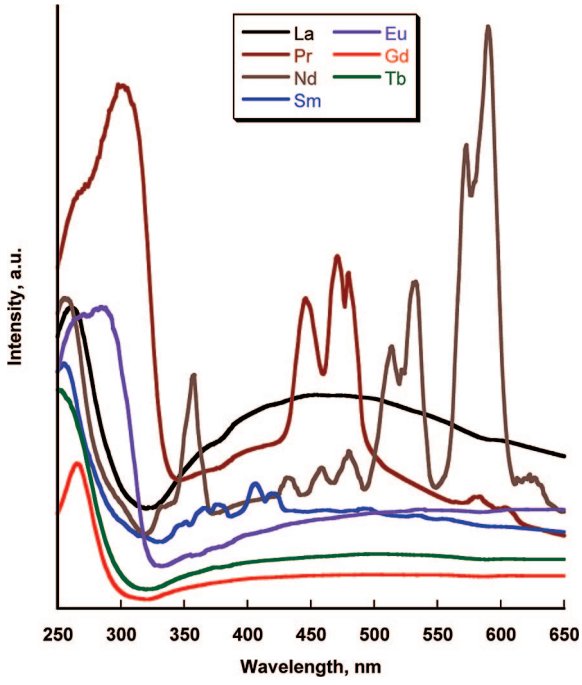

Figure 6. UV−vis diffuse reflectance spectra of $LnKNaNbO_5$ (Ln = La, Pr, Nd, Sm, Eu, Gd, Tb).

The size imposed stability limit of the $LnKNaNbO_5$ series lies at the Tb analogue. Any attempts to synthesize other members of the series containing smaller lanthanides failed. Unfortunately, even though crystals of $TbKNaNbO_5$ were obtained from the hydroxide flux, the crystals that were obtained were too small to be suitable for single crystal X-ray diffraction. In addition, perhaps because the $TbKNaNbO_5$ composition lies at the instability boundary, the powder synthesis inevitably resulted in a two-phase mixture, namely, $TbKNaNbO_5$, and what appears to be Tb_3NbO_7, which has been reported previously[35,36]. We decided to carry out a *Le Bail* profile fit, which confirmed that $TbKNaNbO_5$ crystallizes in the same space group as the other members in the series, *P*4/*nmm,* with lattice parameters $a = 5.6504(5)$ Å and $c = 8.2077(3)$ Å.

It is perhaps not surprising that the stability limit occurs at the terbium analogue, as it is well-known that the size and hence coordination number preference of the lanthanides decreases from lanthanum to lutetium. The early lanthanides prefer coordination numbers of 8 or greater, while the later lanthanides are often found in a 6-fold environment. As the $LnKNaNbO_5$ structure requires an 8-fold coordination environment for the lanthanide cation, we would anticipate that it will not form for the later (smaller) lanthanides. To estimate where the structural stability limit lies, we can look at interlanthanide structures of the type $LnLn'O_3$ for guidance, where as a function of lanthanide size the ABO_3 perovskite, the A-Ln_2O_3, the B-Ln_2O_3, or the C-Ln_2O_3 structures form.[37] In this family of compounds, for many compositions a structure transition is observed to take place near gadolinium, where

(33) *SHELXTL*, Version 6.14; Bruker Analytical X-ray Systems, Inc.: Madison, WI, 2000.
(34) Mugavero, S. J., III; Gemmill, W. R.; zur Loye, H.-C. *J. Solid State Chem.*, submitted.
(35) Doi, Y.; Harada, Y.; Hinatsu, Y. *J. Solid State Chem.* **2009**, *182*, 709.
(36) Wakeshima, M. H. N.; Hinatsu, Y. *J. Phys.: Condens. Matter* **2004**, *16*, 4103.
(37) Bharathy, M.; Fox, A. H.; Mugavero, S. J.; zur Loye, H.-C. *Solid State Sci.* **2009**, *11*, 651.

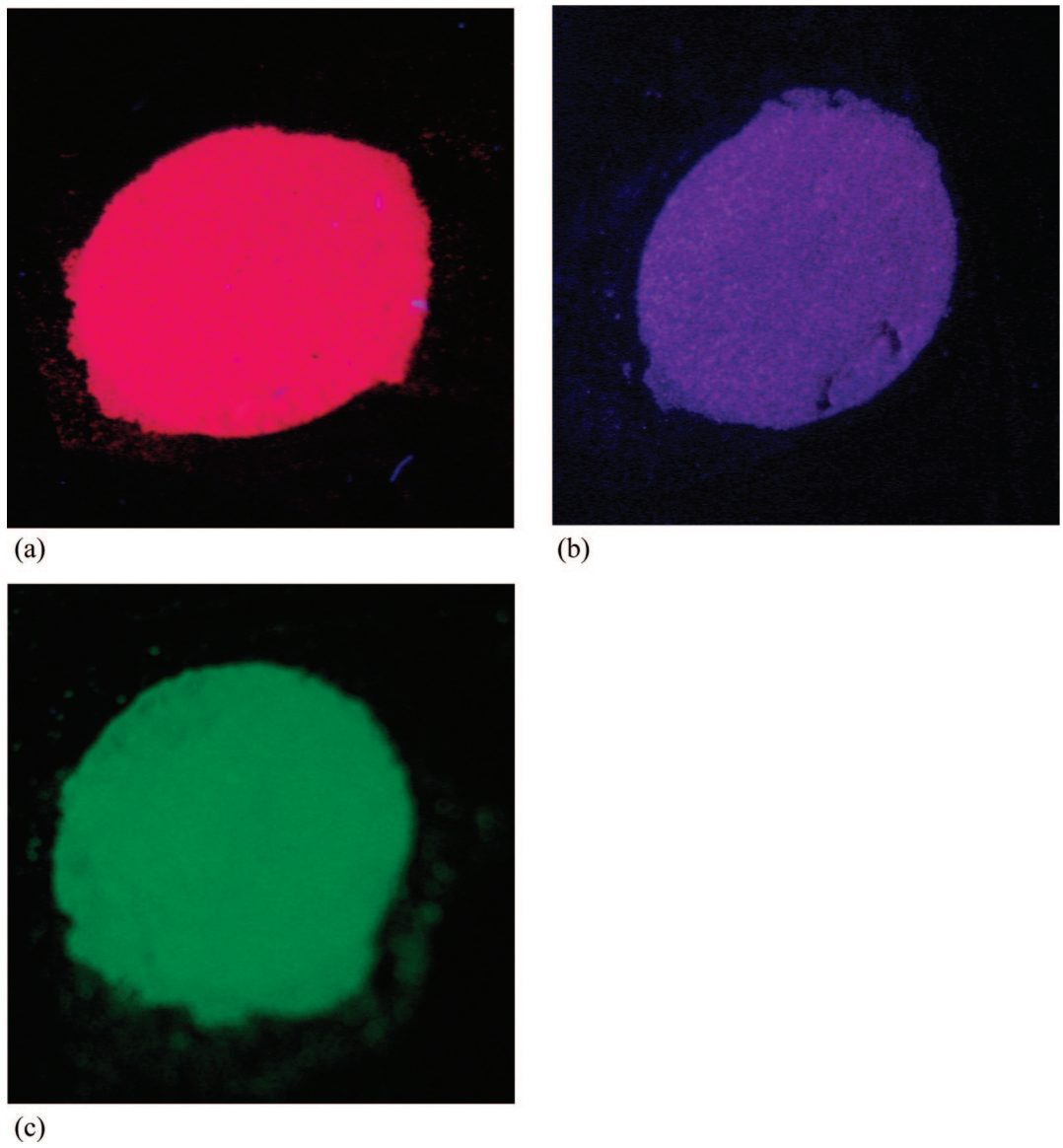

Figure 7. Optical images of (a) $EuKNaNbO_5$, (b) $GdKNaNbO_5$, and (c) $TbKNaNbO_5$ under UV irradiation at room temperature.

for the smaller lanthanides the 6-fold coordination environment predominates. In the $LnKNaNbO_5$ structure we observe that the gadolinium analogue forms readily, the terbium analogue forms only with difficulty, and the dysprosium analogue does not form. Looking at the bond valence sums (Table 4) we find that as we go from lanthanum to gadolinium the rare earth cations go from being slightly over-bonded (BVS = 3.1) to slightly under-bonded (BVS = 2.9), which does not, however, provide a compelling reason for the difficulty in preparing the dysprosium analogue. On the other hand dysprosium is quite stable in 6-fold coordination and, apparently, too small to occupy favorably the cubic site in $LnKNaNbO_5$; this is probably the reason why it does not form in this structure type. We can hypothesize that as we move closer to lutetium, we might expect a different stable structure type to form in which the rare earth cation is found in 6-fold coordination.

Photophysical Properties. *UV−Vis.* Figure 6 shows the diffuse-reflectance spectra of ground crystals of all compounds of the series $LnKNaNbO_5$. A large absorption edge is clearly visible in all spectra, corresponding to the energy gap between the valence band (mostly oxygen 2p orbitals) and the empty conduction band (mostly niobium 4d orbitals). It is common to estimate the band gap by the onset of the absorption edge, and the values obtained by this procedure range from 3.5 to 3.9 eV, making these oxides wide band gap semiconductors. As can be seen from the spectra, there does not appear to be a clear dependency of the energy gap on the rare earth present in the structure.

Photoluminescence. The photoluminescence excitation and emission spectra of the three analogues of the series, $EuKNaNbO_5$, $GdKNaNbO_5$, and $TbKNaNbO_5$, were collected to study the bright orange-red, pink-purple, and green emissions, respectively. Figure 7 shows optical images of ground crystals of these three compounds under short UV irradiation (264 nm) for visual comparison. Figure 8 shows room temperature excitation and emission spectra of $EuKNaNbO_5$, $GdKNaNbO_5$, and $TbKNaNbO_5$. The emission peak of the europium compound has its maximum at 610 nm, whereas the maximum of the excitation peak lies at 538 nm. The gadolinium compound shows the most intense emission at 483 nm with excitation at 250 nm. The emission

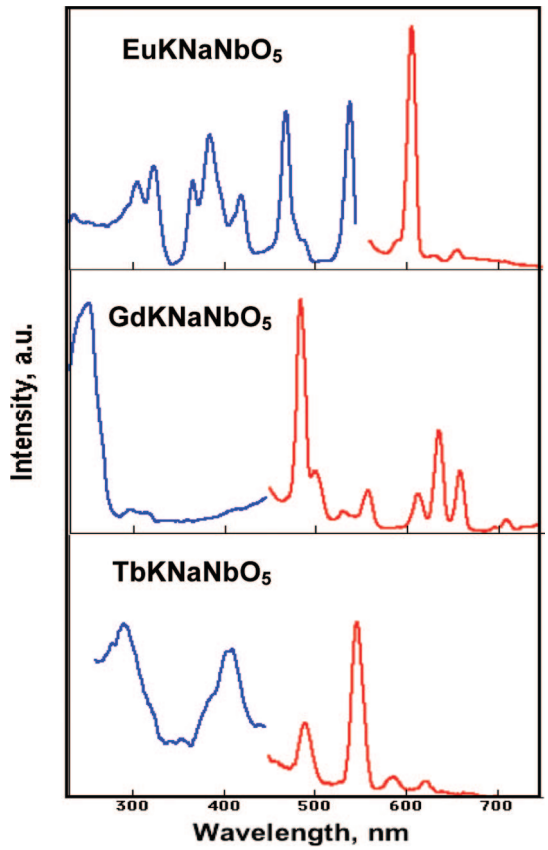

Figure 8. Room temperature photoluminescence spectra of $EuKNaNbO_5$, $GdKNaNbO_5$, and $TbKNaNbO_5$.

peak of the terbium compound has its maximum at 545 nm with the corresponding excitation maximum at 290 nm. The intense room temperature photoluminescence of the $LnKNaNbO_5$ (Ln = Eu, Gd, Tb) is generated by the rare earth cations present in the structure, as the color of the emission changes for different lanthanides. Furthermore, the La, Pr, Nd, and Sm containing members of this family do not exhibit photoluminescence at all, suggesting that the niobate framework is not directly involved in the photoluminescence process but rather that the luminescence originates with the specific rare earth element in the structure. The most intense peak at 607 nm for $EuKNaNbO_5$, 385 and 640 nm for $GdKNaNbO_5$, and 550 nm for $TbKNaNbO_5$ are responsible for the red-orange, pink-purple, and green colors of the luminescence, respectively.

To achieve room temperature photoluminescence, most oxides have to be activated with a photoluminescent ion, such as a trivalent lanthanide,[9,11,17,38] trivalent bismuth,[15] or a combination of ions.[9,38] Photoluminescence activated by doping is strongly dependent on the dopant level, and concentration quenching is typically observed when doping levels exceed 5−10%.[9,15,18,38,39] Interestingly, our materials contain a rare earth ion fully occupying a specific crystallographic site within the structure. This 100% presence might be expected to result in concentration quenching, which, however, clearly is not the case for the materials reported herein. Intrinsic photoluminescence is not very common in inorganic oxides, although it has been reported previously.[16,22] The $LnKNaNbO_5$ structure can, thus, be added to the list of oxide hosts that can support luminescence for some rare earth cations even when they fully occupy a position in the structure, unlike most host structures in which concentration quenching is observed.

4. Conclusions

Single crystals of a series lanthanide containing niobates, $LnKNaNbO_5$ (Ln = La, Pr, Nd, Sm, Eu, Gd, Tb), were synthesized utilizing a low temperature approach using hydroxide melt as well as by solid-state synthesis. The Tb analogue lies at the instability boundary, which led to difficulties in structural refinement due to the extremely small size of the crystals as well as the persistent presence of a second phase in the polycrystalline powders. All members of the family crystallize in a pseudolayered structure containing niobium in an uncommon square pyramidal coordination environment. The Eu, Gd, and Tb members of the series exhibit intense room temperature photoluminescence with bright orange-red, purple-pink, and green emissions, respectively.

Supporting Information Available: Powder X-ray diffraction patterns of XRD for $LnKNaNbO_5$ (Ln = La, Pr, Nd, Sm, Eu, Gd and Tb) (PDF). This material is available free of charge via the Internet at http://pubs.acs.org. Further details of the crystal structure investigations can be obtained from the Fachinformationszentrum Karlsruhe, 76344 Eggenstein-Leopoldshafen, Germany (fax, +49 7247 808 666; e-mail address, crysdata@FIZ-Karlsruhe.de) on quoting the depository numbers CSD-420036, CSD-420037, CSD-420038, CSD-420039, and CSD-420040 for $EuKNaNbO_5$, $GdKNaNbO_5$, $NdKNaNbO_5$, $PrKNaNbO_5$, and $SmKNaNbO_5$, respectively.

Acknowledgment. This work was supported by the National Science Foundation through Grants DMR:0450103 and DMR:0804209.

CM9003245

(38) Hui, Y. Y.; Lin, C.-F. *Mater. Lett.* **2007**, *61*, 3802.

(39) Gasparotto, G.; Lima, S. A. M.; Davolos, M. R.; Varela, J. A.; Longo, E.; Zaghete, M. A. *J. Lumin.* **2008**, *128*, 1606.